

## Synthesis and SAR of p38 $\alpha$ MAP kinase inhibitors based on heterobicyclic scaffolds

T. G. Murali Dhar,\* Stephen T. Wroblewski, Shuqun Lin, Joseph A. Furch, David S. Nirschl, Yi Fan, Gordon Todderud, Sidney Pitt, Arthur M. Doweiko, John S. Sack, Arvind Mathur, Murray McKinnon, Joel C. Barrish, John H. Dodd, Gary L. Schieven and Katerina Leftheris

*Bristol-Myers Squibb Pharmaceutical Research Institute, Princeton, NJ 08543-4000, USA*

Received 22 May 2007; revised 9 July 2007; accepted 9 July 2007

Available online 21 July 2007

**Abstract**—The synthesis and structure–activity relationships (SAR) of p38 $\alpha$  MAP kinase inhibitors based on heterobicyclic scaffolds are described. This effort led to the identification of compound (**21**) as a potent inhibitor of p38 $\alpha$  MAP kinase with good cellular potency toward the inhibition of TNF- $\alpha$  production. X-ray co-crystallography of an oxalamide analog (**24**) bound to unphosphorylated p38 $\alpha$  is also disclosed.

© 2007 Elsevier Ltd. All rights reserved.

A significant body of the literature has underscored the importance of proinflammatory cytokines TNF- $\alpha$  and IL-1 $\beta$  as important mediators in the pathophysiology of chronic inflammatory diseases like rheumatoid arthritis, Crohn's disease, and psoriasis.<sup>1</sup> The regulatory approval and clinical success of anti-cytokine biological agents anakinra (Kineret),<sup>2</sup> an IL-1 receptor antagonist, etanercept (Enbrel),<sup>3</sup> a soluble TNF receptor fusion protein, infliximab (Remicade),<sup>4</sup> and adalimumab (Humira), both TNF- $\alpha$  monoclonal antibodies, has validated the concept of inhibiting proinflammatory cytokines in the treatment of chronic inflammatory diseases. This has sparked significant effort in both academia and industry to identify orally bioavailable small molecule inhibitors of TNF- $\alpha$  and IL-1 $\beta$  reduction.<sup>5</sup>

The mitogen-activated protein kinase (MAPK) p38 is one of the most extensively studied kinase partly because of its important role as a key enzyme in the production of proinflammatory cytokines such as TNF- $\alpha$  and IL-1 $\beta$ .<sup>6</sup> Of the four different isoforms of the p38 family ( $\alpha$ ,  $\beta$ ,  $\gamma$ , and  $\delta$ ), p38 $\alpha$  is ubiquitously expressed and is generally considered the most important isoform in the inflammatory signal transduction pathway and an

appropriate target for anti-inflammatory therapy. Because of this, there has been an intense effort in the pharmaceutical industry to identify safe and effective p38 $\alpha$  inhibitors that has resulted in the identification of several clinical compounds.<sup>7</sup> We recently disclosed a series of 5-cyanopyrimidines and pyrrolo[2,1-*f*][1,2,4]triazines as novel inhibitors of the p38 $\alpha$  MAP kinase.<sup>8</sup> This letter describes the synthesis and preliminary structure–activity relationships (SAR) of p38 $\alpha$  inhibitors based on a heterobicyclic scaffold (A) as depicted in Figure 1.

Figure 1 outlines the rationale for the synthesis of heterobicyclic p38 $\alpha$  inhibitors. Scios recently reported the synthesis and structure–activity relationships (SAR) of indole based heterocyclic inhibitors of p38 $\alpha$ .<sup>9</sup> The authors initially identified compound (**1**) as a submicromolar inhibitor of p38 $\alpha$ . They hypothesized that the introduction of methyl groups on the piperidine ring of compound (**1**) would restrict conformational mobility and potentially lead to analogs with increased potency. Based on this rationale compound (**2**) was synthesized and was found to be ~14-fold more potent than compound (**1**) as shown in Figure 1.

Further modifications to the indole scaffold eventually led to Scios's first p38 clinical compound, Scios-469.<sup>10</sup>

In our recent efforts focused on designing novel classes of p38 inhibitors, we envisioned that incorporation of

**Keywords:** p38 $\alpha$ ; MAP kinase inhibitors; TNF $\alpha$ ; X-ray co-crystallography.

\* Corresponding author. Tel.: +1 609 252 4158; fax: +1 609 252 7410; e-mail: [murali.dhar@bms.com](mailto:murali.dhar@bms.com)

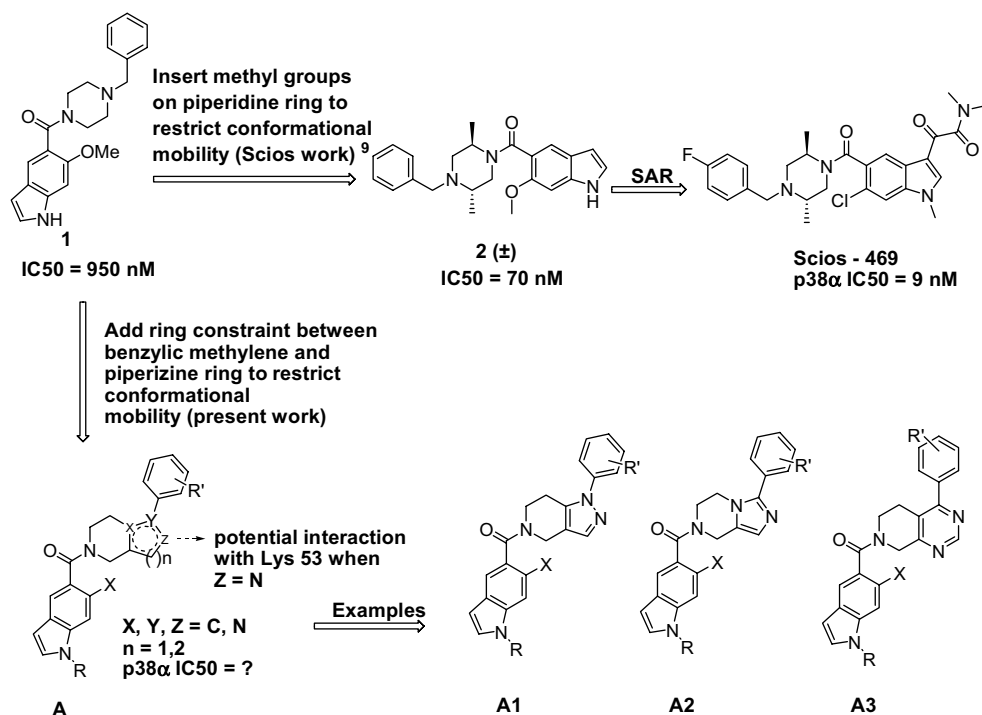
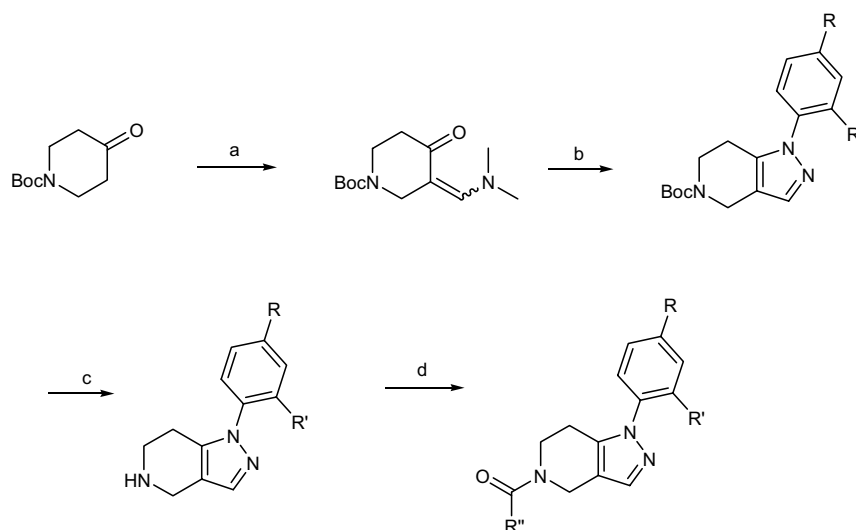


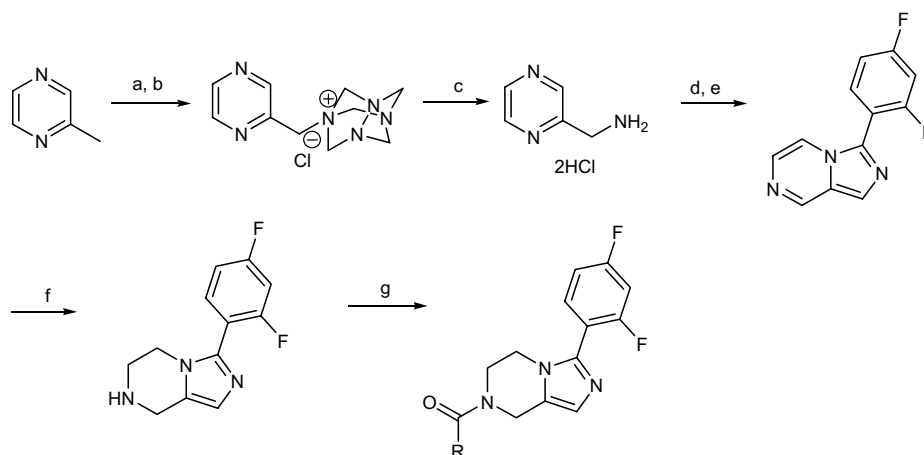
Figure 1.

a ring constraint between the benzyl methylene position and a proximal piperazine or piperidine ring as depicted in compounds of type **A** 1–3 (Fig. 1) would also decrease conformational mobility, and potentially lead to a novel series of heterobicyclic p38α inhibitors. Molecular modeling studies suggested that this type of ring constraint may be advantageous for two main reasons: (1) to lock the terminal aryl group in a conformation favorable for occupying the deep hydrophobic pocket of p38α as defined by amino acids Thr106, Lys53, Leu75, Leu86, Leu104, and Val105; (2) to allow the possibility of pick-

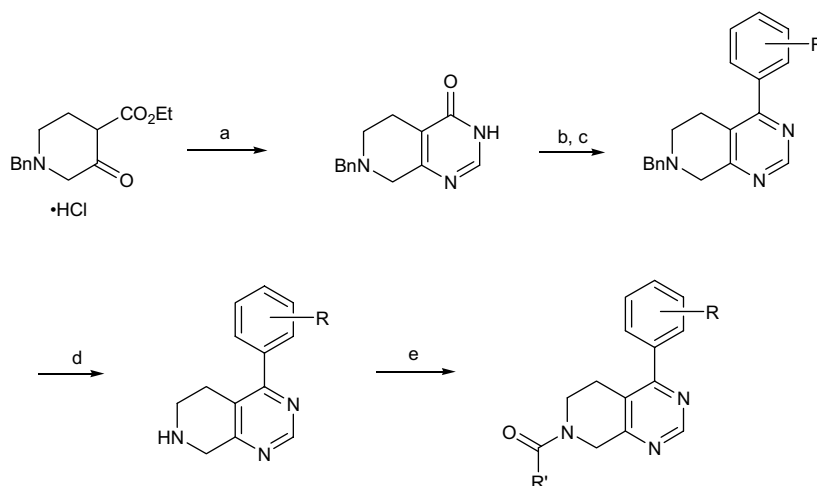
ing up an additional favorable H-bond to Lys53 via a nitrogen atom in compounds of type **A** 1–3 (when Z = N). Based on this rationale we chose to synthesize the pyrazolo[4,3-*c*]pyridine (**A1**), imidazo[1,5-*a*]pyrazine (**A2**), and pyrido[3,4-*d*]pyrimidine (**A3**) for further evaluation. The synthesis of scaffolds **A1**, **A2**, and **A3** is outlined in Schemes 1–3. Since the synthesis of the imidazo[1,5-*a*]pyrazine core (**A2**) incorporates a hydrogenation step, only fluorine substituents were employed on the phenyl moiety that was designed to project into the deep hydrophobic pocket.



**Scheme 1.** Reagents and conditions: (a) *tert*-butoxy bis(dimethylamino)methane, 110 °C, 16 h (46%); (b) subst. or unsubst. phenylhydrazine, AcOH, aq MeOH, rt, 1 h (~50–70%); (c) anhyd HCl, dioxane, 40 °C, 2 h (quantitative); (d) R'COCl, CH<sub>2</sub>Cl<sub>2</sub>, (iPr)<sub>2</sub>EtNH<sub>2</sub>, rt, 0.5 h.



**Scheme 2.** Reagents and conditions: (a) NCS,  $\text{CCl}_4$ ,  $(\text{C}_6\text{H}_5\text{CO})_2\text{O}_2$ , reflux 20 h; (b) hexamethylenetetramine (HMTA), toluene,  $100^\circ\text{C}$ , 20 h (62% for steps a, b); (c) EtOH, concd HCl, reflux 6 h, rt, 85 h; (d) 2,4-difluorobenzoyl chloride,  $(i\text{-Pr})_2\text{EtNH}_2$ , dioxane, DMF, rt, 18 h (65%); (e)  $\text{POCl}_3$ ,  $110^\circ\text{C}$ , 4 h (40%); (f)  $\text{H}_2$ , 10% Pd-C, MeOH, 40 psi, 20 h (quantitative); (g)  $\text{RCOCl}$ ,  $\text{CH}_2\text{Cl}_2$ ,  $(i\text{-Pr})_2\text{EtNH}_2$  or  $\text{RCO}_2\text{H}$ , DMF, BOP,  $\text{Et}_3\text{N}$ .



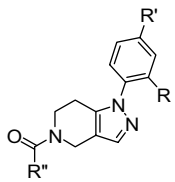
**Scheme 3.** Reagents and conditions: (a) formamidine acetate, NaOMe, MeOH, rt, 20 h (70%); (b)  $\text{POCl}_3$ ,  $(i\text{-Pr})_2\text{EtNH}_2$ , toluene,  $105^\circ\text{C}$ , 2 h (99%); (c) subst. or unsubst. boronic acid or ester, 2 M aq  $\text{K}_2\text{CO}_3$ ,  $\text{Pd}(\text{PPh}_3)_4$ , EtOH/toluene (~1:9),  $110^\circ\text{C}$ , 10 h; (d) 1-chloroethylchloroformate,  $(i\text{-Pr})_2\text{EtNH}_2$ ,  $\text{CH}_2\text{Cl}_2$ ,  $0^\circ\text{C}$  to rt, 20 h.

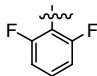
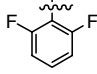
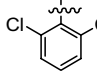
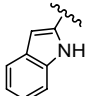
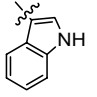
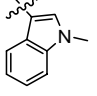
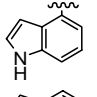
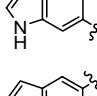
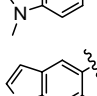
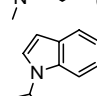
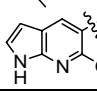
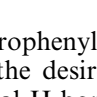
The indole carboxylic acids required to synthesize the corresponding carboxamide analogs were either commercially available or were prepared by methods known in the literature.<sup>11</sup>

The preliminary SAR for the pyrazolo[4,3-*c*]pyridine (**A1**) and imidazo[1,5-*a*]pyrazine (**A2**) are outlined in Tables 1 and 2, respectively.

Although the initial compounds tested in this series were moderately potent inhibitors of p38 $\alpha$ ,<sup>12</sup> we were pleased to see that many of the indole based analogs (**7–13** Table 1) achieved potencies similar to compound **2**, thus supporting our aforementioned hypothesis of conformational restriction of the piperidine ring via ring fusion (Fig. 1). In addition, SAR trends that appear to diverge from previously reported<sup>9</sup> SAR in the compound **2** series were also observed. First, whereas analogs of **2** appear to require a combination of the dimethyl groups on the piperazine ring and a substituent on the 6-position

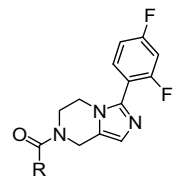
of the indole ring for optimal potency, the initial trends with the pyrazolo[4,3-*c*]pyridine (Table 1) suggested that incorporation of a substituent at the 6-position of the indole ring did not significantly alter the potency in this series (e.g., compare **11** with **12**, Table 1). Second, C-3, C-4, and C-6 substituted indole carboxamides (Table 1, analogs **7**, **9**, and **10**, respectively) were nearly equipotent in the p38 $\alpha$  enzyme assay (40–55 nM). This result is in contrast to the piperazine amides related to **2** where the C-3, C-4, and C-6 substituted indole carboxamides displayed decreased potencies (1.5–4.7  $\mu\text{M}$ )<sup>9</sup> in the enzyme assay. Only the C-2 substituted indole isomer **6** in the pyrazolo[4,3-*c*]pyridine series appeared significantly less active (~4- to 5-fold) than the corresponding C-3, C-4, and C-6 substituted indole carboxamide analogs. These results suggest that incorporation of the ring constraint as outlined in Figure 1 leads to analogs that are more tolerant to amide substituent modifications relative to the piperazine amide series. This observation may be due to a combination of conformational restric-

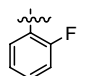
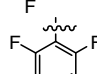
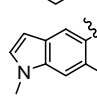
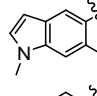
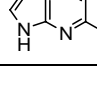
**Table 1.** Pyrazolo[4,3-*c*]pyridine (**A1**) SAR


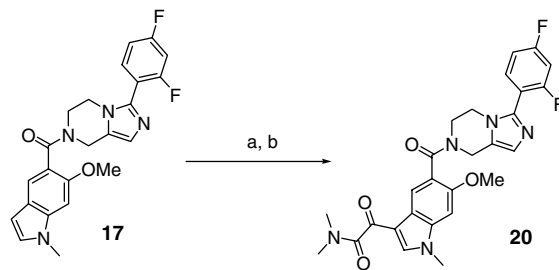
Compound	R, R'	R''	P38 $\alpha$ C <sub>50</sub> (nM)
3	Cl, F		97
4	Cl, H		68
5	Cl, H		112
6	Cl, H		154
7	Cl, H		55
8	Cl, H		40
9	Cl, H		37
10	Cl, H		40
11	Cl, H		30
12	Cl, H		26
13	Cl, H		39
14	Cl, H		137

tion that forces the chlorophenyl moiety to occupy the hydrophobic pocket in the desired orientation as well as the potential additional H-bond interaction between the pyrazole N-2 nitrogen and the Lys53 residue (*vide infra*).

In order to further improve the potency within the pyrazolo[4,3-*c*]pyridine (**A1**) and imidazo[1,5-*a*]pyrazine (**A2**) series, we decided to investigate the SAR of indole based analogs which incorporate an oxalamide side chain at the C-3 position due to the recent disclosure of related oxalamides as potent inhibitors of p38 $\alpha$ .<sup>10</sup> Installation of the oxalamide side chain was undertaken as described in the conversion of **17**–**20** (Scheme 4). A

**Table 2.** Imidazo[1,5-*a*]pyrazine (**A2**) SAR


Compound	R	P38 $\alpha$ C <sub>50</sub> (nM)
15		593
16		167
17		38
18		50
19		164

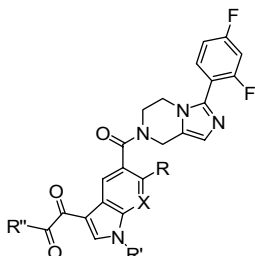
**Scheme 4.** Reagents and conditions: (a) (COCl)<sub>2</sub>, CH<sub>2</sub>Cl<sub>2</sub>, rt, 30 min; (b) dimethylamine (2.0 M in THF), 0 °C (52% for steps a, b).

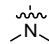
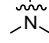
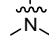
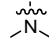
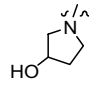
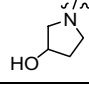
similar sequence was employed for the preparation of the pyrazolo[4,3-*c*]pyridine **26** and **27** and the pyrido[3,4-*d*]pyrimidine analog **28**.

The SAR for the indole based pyrazolo[4,3-*c*]pyridines (**A1**), imidazo[1,5-*a*]pyrazines (**A2**), and pyrido[3,4-*d*]pyrimidines (**A3**) having an oxalamide moiety at the C-3 position is outlined in Table 3 and Figure 2.

As is evident from Table 3 and Figure 2, incorporation of the oxalamide side chain at the C-3 position of the indole moiety improves the p38 $\alpha$  enzyme potency in both the pyrazolo[4,3-*c*]pyridine (**A1**) and imidazo[1,5-*a*]pyrazine (**A2**) series 3- to 10-fold (e.g., compare **14** in Table 1 with **26a** in Figure 2, and **18** in Table 2 with **22** in Table 3). Consistent with the SAR outlined earlier for the pyrazolo[4,3-*c*]pyridine, the deschloro analog **27** is equipotent to compound **26b** (Fig. 2).

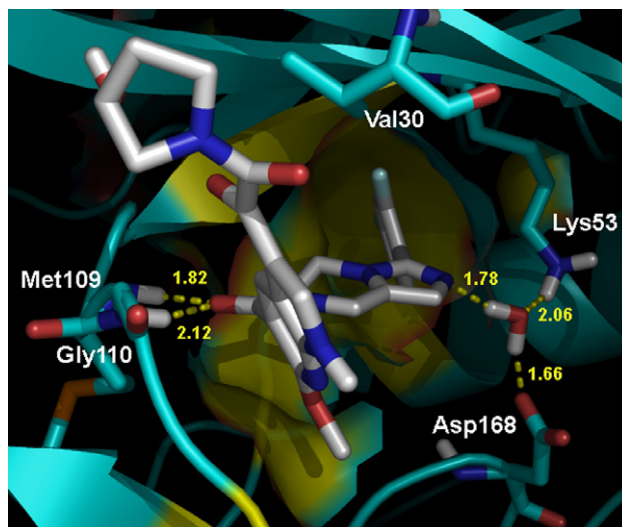
To understand the binding mode of the pyrazolo[4,3-*c*]pyridine (**A1**) and imidazo[1,5-*a*]pyrazine (**A2**) class of p38 $\alpha$  inhibitors we performed X-ray co-crystallo-

**Table 3.** Imidazo[1,5-*a*]pyrazine (**A2**) SAR with oxalamide side chain


Compound	X	R	R'	R''	P38α C <sub>50</sub> (nM)
<b>20</b>	CH	OMe	Me		13
<b>21</b>	CH	Cl	H		11
<b>22</b>	CH	Cl	Me		14
<b>23</b>	N	OMe	H		29
<b>24(±)</b>	N	OMe	H		13
<b>25(±)</b>	N	OMe	Me		16

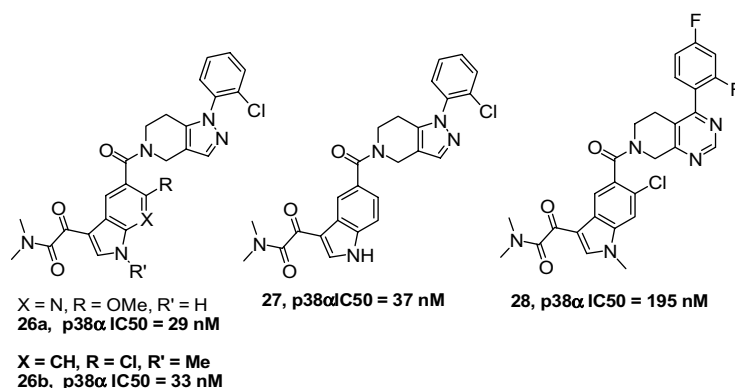
graphic studies of compound **24** (Table 3) with purified, unphosphorylated p38α. The key binding interactions between compound **24** and the p38α enzyme are illustrated in Figure 3.<sup>13</sup>

The X-ray structure of **24** complexed with p38α reveals a combination of H-bonding and hydrophobic interactions. The hinge region residues, Met109 and Gly110, form H-bonds between their backbone NHs and the central amide carbonyl of the inhibitor. The exposed imidazo nitrogen of the inhibitor engages in a H-bond to a water molecule which is itself H-bonded to Lys53 and Asp168. The pendant 2,4-difluorophenyl group is located in a deep hydrophobic cavity flanked by the

**Figure 3.** Binding interactions between **24** and unphosphorylated p38α based on X-ray crystallographic analysis (1.7 Å resolution). Hydrogen bond distances are given in angstroms with key protein residues labeled.

gatekeeper residue Thr106 (not shown) and the carbon chain of Lys53. The inner walls of the cavity are made up of Leu75, Leu86, Leu104, and Val 105. The methoxy moiety sits in a shallow cavity formed by Ile84 and Ala157. The terminal oxalamide appears to extend into solvent and does not engage in any specific interaction with the protein. However, a close inspection of the binding site in contact with the oxalamide group reveals that, although there are no specific H-bonds between protein and the oxalamide moiety, the group fits into a shallow hydrophobic groove on the surface made up of P-loop Val30 and hinge region Leu108/Gly110. Effectively, this interaction results in changing the exposed surface of the protein–ligand complex (in the contact region) from hydrophobic to hydrophilic. The end result is a modest hydrophobic effect wherein binding affinity may be enhanced by the removal of ordered solvent water molecules at the lip of the binding site.

Although incorporation of the oxalamide side chain contributed to a 3- to 10-fold boost in potency in the pyrazolo[4,3-*c*]pyridine (**A1**) and imidazo[1,5-*a*]pyrazine

**Figure 2.** Pyrazolo[4,3-*c*]pyridine (**A1**) and pyrido[3,4-*d*]pyrimidine (**A3**) SAR with oxalamide side chain.



(A2) series, the corresponding pyrido[3,4-*d*]pyrimidine analog **28** was significantly less potent (Fig. 2). In light of the aforementioned X-ray co-crystal structure for the imidazo[1,5-*a*]pyrazine analog **24**, this result was surprising since all key interactions of compound **28** with the enzyme appear to be in place for optimal potency. A plausible explanation could be that the H-bonding trajectory of either the imidazo or pyrazolo nitrogens toward the available water molecule held by Asp168/Lys53 is not reproduced when the nitrogen is in a pyrimidine ring. In the former case, the plane of interaction is in line with the water (OH) and is about 1.7 Å in length (based on the X-ray structure). When the pyrimidine analog was modeled, the resulting trajectory is significantly off-plane and the distance increases to 2.1 Å. Thus, the pyrimidine core offers a less efficient H-bonding opportunity to this water molecule.

In conclusion, we have identified novel series of pyrazolo[4,3-*c*]pyridine (A1), imidazo[1,5-*a*]pyrazine (A2) and pyrido[3,4-*d*]pyrimidine (A3)-based p38 $\alpha$  inhibitors. Incorporation of an oxalamide moiety at the C-3 position of the indole significantly improved the enzyme potency in these series. One of the compounds was a potent inhibitor of TNF- $\alpha$  release (compound **21**, Table 3, IC<sub>50</sub> = 460 nM) in human peripheral blood mononuclear cells (PBMCs).<sup>14</sup>

### Acknowledgments

The authors thank their colleagues Susan E. Kiefer, John A. Newitt, and Kevin Kish for their efforts in expressing and purifying p38 $\alpha$  protein and producing p38 $\alpha$  co-crystals with compound **24** that were used in this study.

### References and notes

- Wagner, G.; Laufer, S. *Med. Res. Rev.* **2006**, *26*, 1.
- (a) Kavanaugh, A. *Adv. Ther.* **2006**, *23*, 208; (b) Fleischmann, R. *Expert Rev. Clin. Immunol.* **2006**, *2*, 331.
- Grunke, M.; Kalden, J. R. *Expert Rev. Clin. Immunol.* **2005**, *1*, 313.
- (a) Saleem, B.; Mackie, S.; Emery, P. *Expert Rev. Clin. Immunol.* **2006**, *2*, 193; (b) Cottone, M.; Mocciano, F.; Modesto, I. *Expert Opin. Biol. Ther.* **2006**, *6*, 401.
- For reviews of this area see: (a) Hynes, J., Jr.; Leftheris, K. *Curr. Top. Med. Chem.* **2005**, *5*, 967; (b) Goldstein, D. M.; Gabriel, T. *Curr. Top. Med. Chem.* **2005**, *5*, 1017; (c) Diller, D. J.; Lin, T. H.; Metzger, A. *Curr. Top. Med. Chem.* **2005**, *5*, 953; (d) Dominguez, C.; Powers, D. A.; Tamayo, N. *Curr. Opin. Drug Discov. Dev.* **2005**, *8*, 421; (e) Wagner, G.; Laufer, S. *Med. Res. Rev.* **2006**, *26*, 1.
- (a) Adams, J. L.; Badger, A. M.; Kumar, S.; Lee, J. C. *Prog. Med. Chem.* **2001**, *38*, 1; (b) Lee, J. C.; Laydon, J. T.; McDonnell, P. C.; Gallagher, T. F.; Kumar, S.; Green, D.; McNulty, D.; Blumenthal, M. J.; Heyes, J. R. *Nature* **1994**, *372*, 739.
- (a) Goldstein, D. M.; Gabriel, T. *Curr. Top. Med. Chem.* **2005**, *5*, 1017; (b) Dominguez, C.; Powers, D. A.; Tamayo, N. *Curr. Opin. Drug Discov. Dev.* **2005**, *8*, 421.
- (a) Liu, C.; Wroblewski, S. T.; Lin, J.; Ahmed, G.; Metzger, A.; Wityak, J.; Gillooly, K. M.; Shuster, D. J.; McIntyre, K. W.; Pitt, S.; Shen, D. R.; Zhang, R. F.; Zhang, H.; Doweiko, A. M.; Diller, D.; Henderson, I.; Barrish, J. C.; Dodd, J. H.; Schieven, G. L.; Leftheris, K. *J. Med. Chem.* **2005**, *48*, 6261; (b) Hynes, J., Jr.; Dyckman, A. D.; Lin, S.; Wroblewski, S. T.; Wu, H.; Gillooly, K. M.; Lonial, H.; Loo, D.; McIntyre, K. W.; Pitt, S.; Shen, D. R.; Shuster, D. J.; Zhang, X.; Behnia, K.; Marathe, P. H.; Doweiko, A.; Barrish, J.; Dodd, J.; Schieven, G.; Leftheris, K. *J. Med. Chem.*, submitted for publication.
- Mavunkel, B. J.; Chakravarty, S.; Perumattam, J. J.; Luedtke, G. R.; Liang, X.; Lim, D.; Xu, Y.-J.; Laney, M.; Liu, D. Y.; Schreiner, G. F.; Lewicki, J. A.; Dugar, S. *Bioorg. Med. Chem. Lett.* **2003**, *13*, 3087.
- Dugar, S. 7th World Congress on Inflammation, Melbourne, Australia., August 20–24, 2005.
- Dugar, S. WO2004/032874.
- p38 Enzyme assay: the assays were performed in U-bottom 384-well plates. The final assay volume was 30  $\mu$ l prepared from 15  $\mu$ l additions of enzyme and substrates (fluoresceinated peptide FL-IPTSPITTTYFFFKKK-OH and ATP) and test compounds in assay buffer (100 mM Hepes, pH 7.2, 10 mM MgCl<sub>2</sub>, 0.015% Brij35, and 4 mM DTT). The reaction was initiated by the combination of bacterially expressed, activated p38 with substrates and test compounds. The reaction mixture was incubated at room temperature for 60 min and terminated by adding 30  $\mu$ l of 35 mM EDTA to each sample. The reaction mixture was analyzed on the Caliper LabChip 3000 by electrophoretic separation of the fluorescent substrate and phosphorylated product. Inhibition data were calculated by comparison to no enzyme control reactions for 100% inhibition and vehicle-only reactions for 0% inhibition. The final concentrations of reagents in the assays are ATP, 20  $\mu$ M; FL-IPTSPITTTYFFFKKK-OH, 1.5  $\mu$ M; p38, 6 nM; and DMSO, 0.6%.
- PDB deposition number is 2QD9.
- Dyckman, A.; Hynes, J.; Leftheris, K.; Liu, C.; Wroblewski, S. T. WO 090912, 2003, *Chem. Abstr.* **2003**, *139*, 292275.